Functioning of oxidative phosphorylation in liver mitochondria of high-fat diet fed rats

Jolita Ciapaite [a,i,*], Stephan J.L. Bakker [b], Gerco Van Eikenhorst [a], Marijke J. Wagner [a], Tom Teerlink [c], Casper G. Schalkwijk [d], Mariann Fodor [e], D. Margriet Ouwens [f], Michaela Diamant [g], Robert J. Heine [g], Hans V. Westerhoff [a,h], Klaas Krab [a]

[a] Department of Molecular Cell Physiology, Institute for Molecular Cell Biology, Faculty of Earth and Life Sciences, VU University, Amsterdam, The Netherlands
[b] Department of Internal Medicine, University of Groningen and University Medical Center Groningen, Groningen, The Netherlands
[c] Department of Clinical Chemistry, Institute for Cardiovascular Research, VU University Medical Center, Amsterdam, The Netherlands
[d] Department of Internal Medicine, University Hospital Maastricht, Maastricht, The Netherlands
[e] Departments of Anatomy, Leiden University Medical Center, Leiden, The Netherlands
[f] Molecular Cell Biology, Leiden University Medical Center, Leiden, The Netherlands
[g] Department of Endocrinology, Institute for Cardiovascular Research, VU University Medical Center, Amsterdam, The Netherlands
[h] Manchester Centre for Integrative Systems Biology, MIB, The University of Manchester, UK
[i] Centre of Environmental Research, Faculty of Nature Sciences, Vytautas Magnus University, Kaunas, Lithuania

Abstract

We proposed that inhibition of mitochondrial adenine nucleotide translocator (ANT) by long chain acyl-CoA (LCAC) underlies the mechanism associating obesity and type 2 diabetes. Here we test that after long-term exposure to a high-fat diet (HFD): (i) there is no adaptation of the mitochondrial compartment that would hinder such ANT inhibition, and (ii) ANT has significant control of the relevant aspects of oxidative phosphorylation. After 7 weeks, HFD induced a $24 \pm 6\%$ increase in hepatic LCAC concentration and accumulation of the oxidative stress marker N^ε-(carboxymethyl)lysine. HFD did not significantly affect mitochondrial copy number, oxygen uptake, membrane potential ($\Delta\psi$), ADP/O ratio, and the content of coenzyme Q_9, cytochromes b and $a+a_3$. Modular kinetic analysis showed that the kinetics of substrate oxidation, phosphorylation, proton leak, ATP-production and ATP-consumption were not influenced significantly. After HFD-feeding ANT exerted considerable control over oxygen uptake (control coefficient $C=0.14$) and phosphorylation fluxes ($C=0.15$), extra- ($C=0.23$) and intramitochondrial ($C=-0.56$) ATP/ADP ratios, and $\Delta\psi$ ($C=-0.11$). We conclude that although HFD induces accumulation of LCAC and N^ε-(carboxymethyl)lysine, oxidative phosphorylation does not adapt to these metabolic challenges. Furthermore, ANT retains control of fluxes and intermediates, making inhibition of this enzyme a more probable link between obesity and type 2 diabetes.
© 2006 Elsevier B.V. All rights reserved.

1. Introduction

A diet rich in fat has been shown to induce impaired insulin-stimulated glucose uptake [1], hyperinsulinemia [2], and to lead to development of obesity, type 2 diabetes [3], nonalcoholic fatty-liver disease [4], and atherosclerosis [5] in the long-term. The increased availability of circulating fatty acids to non-adipose tissues regulating glucose homeostasis (skeletal and cardiac muscle, liver, pancreas) in response to high-fat feeding contributes to accumulation of intracellular triacylglycerols and other fatty acid products (i.e. diacylglycerol, long chain acyl-CoA esters (LCAC), ceramide) [4,6]. These lipid metabolites can adversely affect a wide variety of metabolic pathways leading to decreased intracellular glucose oxidation [7], impaired insulin signaling [7] and increased oxidative stress [8].

High-fat diets have been linked to changes in the fatty acid composition and therewith the fluidity of plasma and intracellular membranes [9], which in turn affect their passive permeability to protons [10] as well as the distribution and dimerization of receptors, activities of mitochondrial membrane-bound enzymes [11–13] and the content of coenzyme Q [14]. Mitochondrial function is essential for cellular energy metabolism, the production of reactive oxygen species (ROS), and therefore important for the management of cell life and death. Impaired mitochondrial function is emerging as a factor in insulin resistance, obesity and type 2 diabetes [15–17]. Yet, there have been few studies that ascertained the precise nature and pinned down the molecular mechanism(s) of this dysfunction.

Increased intracellular availability of lipids can lead to increased concentrations of LCAC, molecules that control several aspects of cell function including activation of certain types of protein kinase C, modulation of enzyme activities, protein acylation, ceramide- and/or nitric oxide-mediated apoptosis, and binding to nuclear transcriptional factors (reviewed in [18]). We hypothesized that besides the multitude of the above mentioned effects LCAC may contribute to the mitochondrial and cellular dysfunction in obesity and type 2 diabetes due to persistent partial inhibition of the mitochondrial adenine nucleotide translocator (ANT). On one hand this inhibition is expected to result in decreased cytosolic ATP/ADP ratios, increased levels of cytosolic AMP and adenosine, and on the other hand it may lead to increased mitochondrial membrane potential ($\Delta\psi$) and the redox state of coenzyme Q, causing increased ROS production and oxidative stress [19,20]. We have shown recently that ANT is the only target of palmitoyl-CoA in liver mitochondria from non-obese rats and that inhibition of ANT leads to the predicted changes in ATP/ADP ratios and $\Delta\psi$ [21] as well as increased production of H_2O_2 [22].

However, next to the direct effect on the ANT, LCAC could reprogram gene expression and alter the biochemical composition or abundance of the mitochondria in long-term; therefore here we test this possibility. Furthermore, the control exerted by the target of LCAC, i.e. the ANT over various facets of mitochondrial function could decrease in response to sustained lipid oversupply (e.g. induced by a high-fat diet) making the proposed mechanism [19,20] less probable. In this paper we therefore assess whether also after a high fat diet feeding ANT exerts significant control over various functional properties of mitochondrial oxidative phosphorylation, notably those that correlate with AMP and ROS production (such as extramitochondrial ATP/ADP ratio and $\Delta\psi$).

To this end, rats were exposed for 7 weeks to either a high-fat diet (HFD) or a low fat diet (LFD). We then examined the effects on (i) abundance, properties and functioning of mitochondria and (ii) control of this functioning by ANT. Our data show that HFD feeding causes accumulation of LCAC in liver but has no effect on the mitochondrial compartment.

2. Materials and methods

2.1. Materials

Yeast hexokinase was from Roche (Mannheim, Germany). Oligomycin, myxothiazol, atractyloside, coenzyme Q_9, heptadecanoyl-CoA and P^1,P^5-di(adenoside-5′) pentaphosphate (Ap5A) were obtained from Sigma-Aldrich (Zwijndrecht, The Netherlands).

2.2. Animals and diets

The animal treatment conformed to the Guide for the Care and Use of Laboratory animals published by the US National Institutes of Health (NIH publication no. 85-23, revised 1996) and the guidelines of the Institutional Animal care and Use Committee of the VU University medical center. One group of adult male Wistar rats (302±4.6 g (mean, ±SEM), n=16) were given a low-fat diet (LFD) (Hope Farms, Woerden, The Netherlands, cat #4148.01) containing 8 wt.% of total fat, 22 wt.% protein and 60 wt.% carbohydrate for 7 weeks. The second group (301±3.7 g, n=18) received an isocaloric high-fat diet (HFD) (Hope Farms, Woerden, The Netherlands, cat #4148.02) containing 25 wt.% fat, 32 wt.% protein and 25 wt.% carbohydrate. This way 50.4% of the ingested calories was derived from fat in case of HFD, compared to 16.4% in case of LFD. The percentage of saturated and unsaturated fat was 42.4% and 57.6%, respectively, in both LFD and HFD.

At week 6, rats fasted for 6–8 h received an oral glucose load (2 g/kg of body weight). Blood glucose was measured from tail bleeds with a HemoCue glucose analyser (Angelholm, Sweden) at 120 min after glucose ingestion.

2.3. Isolation of mitochondria

Liver mitochondria were isolated through a standard differential centrifugation procedure as described [23], with 250 mM sucrose, 10 mM Tris–HCl, 3 mM EGTA and 2 mg ml^{-1} BSA (pH 7.7) as the isolation medium. Protein content was determined according to Bradford [24] with bovine serum albumin (BSA) as the standard.

2.4. Measurement of oxygen uptake, $\Delta\psi$ and the ADP/O ratios

In order to simultaneously monitor the oxygen uptake and $\Delta\psi$, mitochondria were incubated at 25 °C in a closed, stirred and thermostated glass vessel equipped with Clark-type oxygen electrode and TPP$^+$-sensitive electrode as described before [21]. The reaction medium contained 25 mM creatine, 25 mM creatine phosphate, 75 mM KCl, 20 mM Tris, 2.3 mM MgCl$_2$, KH$_2$PO$_4$ (5.0 mM), 2 mg ml^{-1} BSA, 10 mM succinate, 2 μM rotenone, 50 μM Ap5A, pH 7.3. An ADP-regenerating system consisting of excess hexokinase (5.78 U ml^{-1}) and glucose (12.5 mM) was used to maintain steady-state respiration rates. 0.1 M of ATP (which would be rapidly converted to ADP by the hexokinase) was added to initiate state 3 respiration.

The ADP/O ratio was determined in reaction medium containing 1 mg of mitochondrial protein ml^{-1} supplemented with 10 mM succinate, 2 μM rotenone and 50 μM Ap5A (to inhibit mitochondrial adenylate kinase) by measuring the amount of oxygen taken up (corrected for proton leak driven respiration [25]) in response to 400 μM ADP as described [26].

2.5. Determination of mitochondrial cytochrome $c+c_1$, b, and $a+a_3$ content

The concentrations of mitochondrial cytochromes $c+c_1$, b and $a+a_3$ were determined from the difference spectra recorded with a modified SLM Aminco DW-2 double-beam dual wavelength spectrophotometer [27]. 20 µl of mitochondrial suspension was added to 1 ml of 20 mM Tris buffer, pH 7.2 and the oxidized spectra were recorded from 500 nm to 650 nm. Reduced spectra were recorded in the same sample after reduction of the cytochromes with solid sodium dithionite. The concentrations of the cytochromes were calculated from the Gaussian deconvolution of the reduced minus oxidized difference spectra [27] using the extinction coefficients: ε_{c+c1}(551–542 nm)=19 mM^{-1} cm^{-1} [28], ε_b (561–572 nm)=20 mM^{-1} cm^{-1} [28], ε_{a+a3}(605–630 nm)=24 mM^{-1} cm^{-1} [29].

2.6. Coenzyme Q_9 measurements

Mitochondrial coenzyme Q_9 was extracted with acidic methanol and petroleum ether and was determined by reverse-phase HPLC using Lichrosorb 10 RP 18 column (4.6 mm×250 mm, Phenomenex) and ethanol/methanol (3:2, v/v) as a mobile phase, flow rate 1 ml min^{-1}, as described in [30]. The oxidized and the reduced coenzyme Q_9 were detected at 275 nm and 290 nm, respectively using a Perkin-Elmer LC 235 diode array detector and the concentrations were calculated from the peak area using coenzyme Q_9 as a standard.

2.7. Determination of the adenine nucleotide concentration

Adenine nucleotides were extracted with phenol as described [31]. The ATP and ADP concentrations in the samples were measured using a luciferin-luciferase ATP monitoring kit (BioOrbit, Turku, Finland). The fractions of ATP in the medium and in the mitochondrial matrix were derived from the hexokinase kinetics as described [21].

2.8. Determination of LCAC concentration in liver

Frozen liver biopsies were rapidly homogenized with five volumes of ice-cold ammonium acetate buffer (100 mM, pH 5.0). Next, 0.27 ml of the homogenate was mixed with 0.03 ml of the internal standard solution (100 µM heptadecanoyl-CoA dissolved in aqueous 10 mM ammonium bicarbonate containing 27% acetonitrile) and 0.6 ml acetonitrile/2-propanol (1/1, v/v). After thorough vortex-mixing, the extract was subjected to a dual centrifugation procedure (2000×g, 10 min, 4 °C, followed by 20,000×g, 30 min). LCAC concentration was determined in the supernatant using liquid chromatography-tandem mass spectrometry (LC-MS/MS) with an API 3000 triple quadruple tandem mass spectrometer (Sciex-Applied Biosystems, Toronto, Canada) interfaced with a TurboIonSpray source. The LC equipment consisted of Series 200 autosampler, quaternary pump and inline degasser (Perkin Elmer, Norwalk, CT, USA). Mass spectra were acquired and processed with Analyst software version 1.3.1 (Sciex-Applied Biosystems). Samples were analyzed at ambient temperature by reversed-phase HPLC with SymmetryShield RP8 column (2.1×100 mm; 3.5 µm particle size; Waters, Milford, MA) using mobile phase consisting of 30% acetonitrile in 2 mM ammonium bicarbonate with a flow rate of 0.2 ml min^{-1}, injection volume 50 µl. Analyses were performed in negative-ion mode, the ion-spray voltage of −4200 V, turbo ion gas temperature 350 °C. The transitions from the doubly charged precursor ions to the singly charged product ions, resulting from collision-induced loss of a phosphate group, were monitored for 50 ms in multiple reaction-monitoring mode. Quantification was based on peak area using C17:0-CoA as internal standard.

The sensitivity (response coefficient) of total hepatic LCAC concentration to change in total fatty acid (FA) concentration in the diet was calculated as:

$$R_{FA}^{LCAC} = \frac{\% \text{ change } [LCAC]_{total}}{\% \text{ change } [FA]_{total}} \tag{1}$$

2.9. Determination of the relative mitochondrial copy number

Genomic DNA was extracted and purified from approximately 30 mg of frozen liver using DNeasy columns (Qiagen, Venlo, The Netherlands). Purity and quantity of extracted DNA was determined spectrophotometrically at 260 and 280 nm. The mitochondrial DNA (mtDNA) content was measured using real-time PCR. Primers for mtDNA were designed using Primer Express software (Applied Biosystems): forward primer -5′-ACACCAAA-AGGACGAACCTG-3′, reverse primer -5′-ATGGGGAAGAAGCCCTA-GAA-3′; and for proliferator-activated receptor-γ coactivator-1α (PGC-1α): forward primer -5′-ATGAATGCAGCGGTCTTAGC-3′, reverse primer -5′-AACAATGGCAGGGTTTGTTC-3′ were published previously [32]. Reactions were carried out in the presence of 1x SYBR® Green PCR Master Mix (4309155, Applied Biosystems), 0.5 µM of each forward and reverse primer, and 50 ng genomic DNA. A standard curve was created using serial dilutions of genomic DNA mixture. Amplifications were performed in an ABI PRISM® 7700 Sequence Detection System with the following cycle conditions: 95 °C for 10 min followed by 40 cycles of 95 °C for 15 min, 60 °C for 30 min, and 72 °C for 30 min. All PCR-reactions were verified by agarose gel electrophoresis. The threshold cycle number (C_t) was calculated using SDS software version 1.9 (Applied Biosystems) and an automated setting of the baseline. The relative mitochondrial copy number (R_c) was determined as described in [33], using the equations:

$$R_c = 2^{\Delta C_t} \tag{2}$$

$$\Delta C_t = C_{t(PGC-1\alpha)} - C_{t(mtDNA)} \tag{3}$$

2.10. Immunohistochemistry

The formalin-fixed paraffin-embedded liver sections (4 µm) were mounted on the microscope slides. The cellular localization of N$^\varepsilon$-(carboxymethyl)lysine (CML) and 4-hydroxy-2-nonenal (HNE) was determined with a monoclonal antibody against CML, (dilution 1:500, v/v) [34] and a monoclonal antibody against HNE (dilution 1:100, v/v) [35] using immunoperoxidase staining with diaminobenzidine as chromogen. Sections from four LFD-fed and six HFD-fed rat livers were analyzed. The staining was evaluated semiquantitatively by assessing each slide at 40× magnification. A staining score was calculated as a score for percentage of positive cells (<25%=1, 26–50%=2, 51–75%=3, >75%=4) multiplied by an intensity score (negative=0, weak=1, moderate=2, strong=3). Thus the highest possible staining score was 12.

2.11. Modular kinetic analysis

In the first application of the analysis, the enzymes of oxidative phosphorylation were conceptually grouped into three functional modules with $\Delta\psi$ as connecting intermediate: (i) substrate oxidation (comprised of dicarboxylate carrier, matrix dehydrogenases and respiratory chain), (ii) phosphorylation module (comprised of phosphate carrier, ATP synthase, ANT and exogenous hexokinase) and (iii) proton leak module (comprised of membrane permeability to protons and cation cycling across the membrane) [25]. In the second application of the analysis the enzymes were grouped into two functional modules with matrix ATP/ADP ratio as connecting intermediate: (i) ATP-producing module (comprised of dicarboxylate carrier, matrix dehydrogenases and respiratory chain, phosphate carrier and ATP synthase) and (ii) ATP-consuming module (comprised of ANT and exogenous hexokinase) [21]. The kinetic response of flux through the modules to changes in the levels of connecting intermediates was determined by titration with module-specific inhibitors as described [25,21].

2.12. Modular metabolic control analysis

The flux (or concentration) control coefficient is a quantitative measure of how important an enzyme is in controlling a pathway flux (or concentration of an intermediate) at steady state (cf. [36]). Effectively it indicates the % reduction in a system flux (or concentration of an intermediate) in response to 1% inhibition of the reaction rate of that enzyme. For metabolic control analysis (MCA), the system of oxidative phosphorylation was divided into five modules (substrate oxidation module, proton leak module, ATP synthesis module, adenine nucleotide translocator and hexokinase) connected by three intermediates ($\Delta\psi$, intra- and extramitochondrial ATP/ADP ratios) (Fig. 1). The control coefficients

of ANT for oxygen uptake (J_o) and phosphorylation (J_p) fluxes and intermediates were calculated from the system fluxes and elasticity coefficients using modular MCA as described [22]. The control coefficient of ANT for $\Delta\psi$ was calculated as described in [37]. Co-response coefficients and elasticity coefficients that were used in the calculations of control coefficients were determined as described in [22] and are given in Supplementary material Tables S.1 and S.2, respectively.

2.13. Data presentation and statistical analysis

Data are expressed as averages, ±SEM. The n values represent the number of independent experiments. Statistical significance of the differences was determined using Student's t-test. A $P<0.05$ that the difference arose by chance was considered to make the difference statistically significant.

3. Results

3.1. High-fat diet causes impaired glucose tolerance

After 7 weeks of exposure to the diets the mean body weight was not significantly different between the two diet groups (468 ± 14 g and 465 ± 12 g for LFD and HFD group, respectively). Fasting glucose levels (6.1 ± 0.3 mM and 6.7 ± 0.1 mM for LFD and HFD group, respectively) were significantly higher ($P<0.05$) in HFD group. Moreover, 2 h post-load blood glucose levels (7.3 ± 0.5 mM and 8.8 ± 0.3 mM for LFD and HFD group, respectively) were significantly higher ($P<0.05$) in HFD group.

3.2. High-fat diet increased hepatic long chain acyl-CoA content

Table 1 shows the LCAC composition in rat-liver following a 7-week LFD- or HFD-feeding. The HFD-feeding resulted in a significant increase in the LCAC content of the liver: the total LCAC concentration was $24\pm6\%$ ($P<0.01$, $n=6$) higher in livers of HFD-fed rats than in livers of LFD-fed rats. This effect was limited when related to the fatty acid content of HFD (the amount of fatty acids in the HFD was three times the amount in the LFD): the average response coefficient was 0.1, reflecting appreciable homeostasis.

HFD (which had the same relative fatty acid composition as the low fat diet) caused slight change of the hepatic LCAC

Table 1
Effect of the diet on long chain acyl-CoA content in liver

Chain length: double bonds	LCAC content in livers				FA content in diets, %
	LFD liver		HFD liver		
	nmol g wet weight^{-1}	%	nmol g wet weight^{-1}	%	
C14:0	0.86±0.07	5.2	0.89±0.03	4.3	0.9
C16:0	1.87±0.2	11.2	2.5±0.14*	12.2	36.9
C16:1	1.57±0.13	9.4	1.16±0.03*	5.6	0.2
C18:0	0.57±0.06	3.4	0.93±0.14*	4.5	3.7
C18:1	5.34±0.29	32.1	7.24±0.46**	35.2	40.6
C18:2	1.7±0.11	10.2	2.75±0.28**	13.4	15.9
C18:3	0.2±0.02	1.2	0.33±0.02**	1.6	0.9
C20:4	4.13±0.39	24.8	4.37±0.25	21.3	(0.6)
C20:5	0.13±0.01	0.8	0.15±0.01*	0.7	
C20:6	0.25±0.02	1.5	0.23±0.02	1.1	
Total	16.63±0.98	100	20.55±0.6**	100	100

Data are averages from $n=6$ rat-livers for each diet group, ±SEM. LFD—low fat diet, HFD—high fat diet, FA—fatty acid. *$P<0.05$, **$P<0.01$ vs. low fat diet.

composition in the direction of that of the diet, but the change was rather limited: the composition remained closer to the composition of the control (LFD) liver than to the HFD composition. The most abundant LCAC-species in both LFD- and HFD-fed rat livers were oleoyl-CoA (C18:1) and arachidonoyl-CoA (C20:4). Especially the latter was much more abundant in the livers than in the diet. More generally, the concentration of long chain acyl-CoA esters containing acyl groups with C20 was much less affected by HFD-feeding compared to the ones with a shorter acyl chain.

3.3. High-fat diet increased protein oxidative stress

We examined whether HFD-feeding led to increased oxidative stress. N$^\epsilon$-(carboxymethyl)lysine (CML) and 4-hydroxy-2-nonenal (HNE) were stained as tissue markers of protein and membrane lipid damage, respectively. Livers from LFD-fed rats only showed mildly positive CML-staining (staining score 0.8 ± 0.3) (Fig. 2A), whereas HFD-feeding caused significant ($P<0.001$) accumulation of CML in the cytosol of hepatocytes
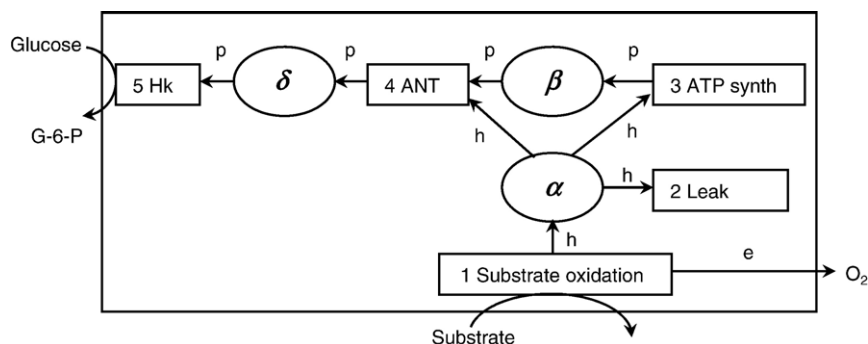
Fig. 1. Division of oxidative phosphorylation into modules. The modules: 1—substrate oxidation module, comprised of dicarboxylate carrier and respiratory chain, 2—proton leak module, comprised of passive membrane permeability to protons and cation cycling across the membrane, 3—ATP synthesis, comprised of ATP synthase and phosphate carrier, 4—adenine nucleotide translocator and 5—hexokinase. The intermediates: α—membrane potential ($\Delta\psi$), β—intramitochondrial ATP/ADP ratio (ATP$_{in}$/ADP$_{in}$), δ—extramitochondrial ATP/ADP ratio (ATP$_{out}$/ADP$_{out}$). Arrows marked e, h and p indicate electron flux, trans-membrane proton flux and ATP flux, respectively. G-6-P—glucose-6-phosphate, Hk—hexokinase, ANT—adenine nucleotide translocator, ATP synth—ATP synthesis.

A

B

Fig. 2. Imunohistochemistry of N^ε-(carboxymethyl)lysine (CML) in livers of low-fat and high-fat diet treated rats. (A) No accumulation o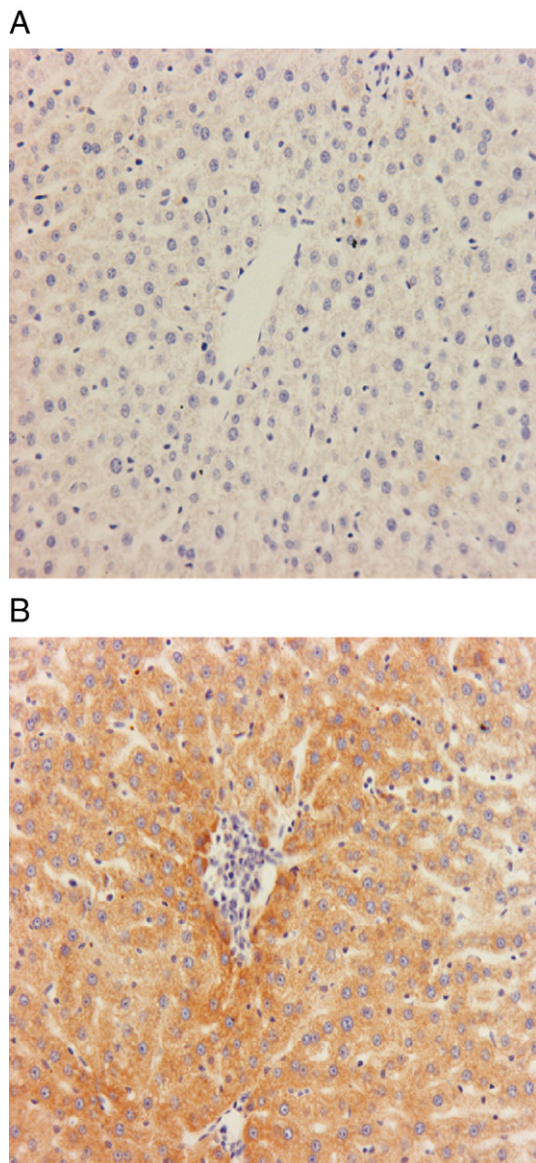f CML in low-fat diet treated rat-livers; (B) high-fat diet treatment causes accumulation of N^ε-(carboxymethyl)lysine in rat-livers. Magnification ×20. Nuclei were stained with Mayer's haematoxylin.

(staining score 9.0 ± 1.0), with areas around the central vein and the portal triad most affected (Fig. 2B). 4-hydroxy-2-nonenal (HNE; a marker of membrane lipid damage) accumulated only slightly the cytosol and in the nuclei of hepatocytes, and this was similar between both diet groups (data not shown).

3.4. High-fat diet hardly affected mitochondrial makeup

Next, we determined how HFD affected the mitochondria. The mitochondrial copy number, as determined by the ratio of mtDNA relative to genomic DNA (PGC-1α gene) did not differ significantly between the livers of LFD- and HFD-fed rats (204 ± 62 ($n=4$) and 221 ± 52 ($n=4$), respectively).

The number of mitochondria being similar, the biochemical composition of the mitochondria could have changed. Table 2 summarizes the content of respiratory chain coenzymes for the two diet groups. There was no significant difference in the content of coenzyme Q_9, cytochrome b and cytochromes $a+a_3$ between the diet groups. The content of the cytochromes $c+c_1$ was $20\pm5\%$ ($P<0.05$) lower in the HFD-treated group.

Although the number of mitochondria was the same in livers from LFD- and HFD-fed rats, the HFD feeding could have increased the respiratory activity of mitochondria. Thus we determined steady-state properties of isolated, actively phosphorylating (state 3) liver mitochondria from HFD- and LFD-fed rats respiring on the TCA-cycle intermediate succinate as the substrate. Table 3 shows that there was no such adaptation either: steady-state oxygen uptake and phosphorylation rate, $\Delta\psi$, the ratio of reduced-to-oxidized coenzyme Q_9, the intra- and extramitochondrial ATP/ADP ratio were all similar between the diet groups. Furthermore, the basal membrane permeability to protons was not changed in mitochondria from HFD-fed rat-livers (Table 3). The efficiency of oxidative phosphorylation expressed as the number of ADP molecules phosphorylated per oxygen atom reduced (ADP/O ratio) was not affected by the diet either (Table 3).

Finally, we examined the functional components of mitochondrial oxidative phosphorylation, through a modular kinetic analysis (cf. [21]). The kinetics of the phosphorylating module (Fig. 3A), substrate oxidation module (Fig. 3B) and the proton leak module (Fig. 3C) were comparable between mitochondria from rats fed LFD and HFD. This is concluded from similar magnitudes of the phosphorylation flux, the oxygen uptake flux and the proton leak flux when compared for any same magnitude of $\Delta\psi$. Modular kinetic analysis with the intramitochondrial ATP/ADP ratio as an intermediate yielded similar kinetics for the ATP-producing module (Fig. 4A), as well as for the ATP-consuming module (Fig. 4B) in the mitochondria in livers of LFD- and HFD-fed rats. This is concluded from the similar fluxes through the modules in both investigated groups at any given matrix ATP/ADP ratio.

3.5. The adenine nucleotide translocator controls mitochondrial function in mitochondria from HFD-fed rats

Our hypothesis requires that ANT have significant control over various properties of mitochondrial oxidative phosphorylation also in conditions of lipid oversupply. We therefore determined the control exerted by ANT in mitochondria isolated from HFD-fed rat livers and compared this control to that in

Table 2
Effect of the diet on the content of the respiratory chain cytochromes and coenzyme Q_9

	Cytochromes, nmol mg protein^{-1}			Co Q_9 pmol. mg protein^{-1}
	$c+c_1$	b	$a+a_3$	
LFD	0.46 ± 0.03	0.30 ± 0.02	0.20 ± 0.01	106.2 ± 10.1
HFD	$0.36\pm0.03*$	0.28 ± 0.03	0.18 ± 0.01	123.9 ± 9.1

Data are expressed as averages from $n=13$ experiments for both diet groups, ±SEM. LFD—low fat diet, HFD—high fat diet. *$P\leq0.05$ vs. low fat diet.

Table 3
Effect of the diet on the steady-state properties of actively phosphorylating (state 3) mitochondria

	LFD	HFD
Oxygen uptake rate, nmol O_2 min^{-1}. mg protein^{-1}	78.0±4.0	73.3±1.0
Phosphorylation rate, nmol ADP min^{-1} mg protein^{-1}	276±10	275±16
Proton leak rate, nmol O_2 min^{-1} mg protein^{-1}	3.2±0.3	3.5±0.3
$\Delta\psi$, mV	153.8±1.3	153.8±1.4
Ratio reduced-to-oxidized Q_9	3.3±0.2	3.8±0.3
Intramitochondrial ATP/ADP ratio	0.59±0.1	0.54±0.1
Extramitochondrial ATP/ADP ratio	0.16±0.02	0.16±0.01
ADP/O ratio	1.75±0.02	1.79+0.04

Data are averages from $n=6$ experiments, ±SEM. LFD—low fat diet, HFD—high fat diet.

liver mitochondria from LFD-fed rats. Table 4 shows the control coefficients of ANT for oxygen uptake (J_o) and phosphorylation (J_p) fluxes, $\Delta\psi$, intra- and extramitochondrial ATP/ADP ratio in liver mitochondria from LFD- and HFD-fed rats. ANT exerted strong control on the intra- and extramitochondrial ATP/ADP ratios, and substantial control over oxygen uptake and phosphorylation fluxes and $\Delta\psi$. Furthermore, the control was retained also after exposure to HFD. The control of intramitochondrial ATP/ADP ratio and $\Delta\psi$ by ANT was negative, since stimulation of ANT activity leads to lower levels of these intermediates.

4. Discussion

We have shown that HFD feeding induced impaired glucose tolerance but did not lead to increased body weight gain in adult rats. HFD caused accumulation of LCAC and the oxidative stress marker N$^\varepsilon$-(carboxymethyl)lysine in liver. However HFD did not alter the number of the mitochondria per cell in the livers and neither the oxidative capacity or efficiency of oxidative

phosphorylation in these mitochondria significantly. Furthermore, ANT exerted significant control on various aspects of oxidative phosphorylation also in the liver mitochondria of the HFD-fed rats.

We previously reported that HFD-feeding induces a glucose intolerant, non-obese phenotype, with accumulation of intracellular triacylglycerols in skeletal muscle and liver ([38], cf. [3]). Here we demonstrate that HFD also causes a significant increase in the concentration of LCAC, the metabolically active form of fatty acids, in liver. Besides being substrates for β-oxidation, LCAC are emerging as important regulators of a variety of biological processes including mitochondrial metabolism [39], insulin secretion and signaling [40]. Furthermore, LCAC were shown to inhibit a number of mitochondrial transport systems including the ANT, dicarboxylate, tricarboxylate and phosphate carriers [41]. However, the observation that LCAC concentration needed to at least partly block di-, tricarboxylate and phosphate carriers would inhibit the ANT completely preventing any activity of oxidative phosphorylation poses a question whether the inhibition of the former carriers is of physiological significance.

In the present study the most obvious increase was observed in LCAC species containing acyl chains with C16:0 and C18 of various degrees of unsaturation, while the content of LCAC with C20 was less affected by HFD. Higher content of C20:4 species in rat-livers compared to that in the diets may be explained by the synthesis of arachidonic acid from its immediate dietary precursor, i.e. linoleic acid (C18:2). In general, strong homeostasis in hepatic LCAC composition was observed, although HFD-induced *changes* in the hepatic LCAC profile partly reflected the dietary fatty acid composition.

To assess whether HFD-feeding can lead to increased oxidative stress we used CML and HNE-protein adducts as markers. CML can arise from both non-enzymatic glycosylation and oxidation of proteins [42] and from metal-catalyzed lipoprotein peroxidation [43], whereas HNE is a product of peroxidative degradation of polyunsaturated membrane lipids [44]. Exposure
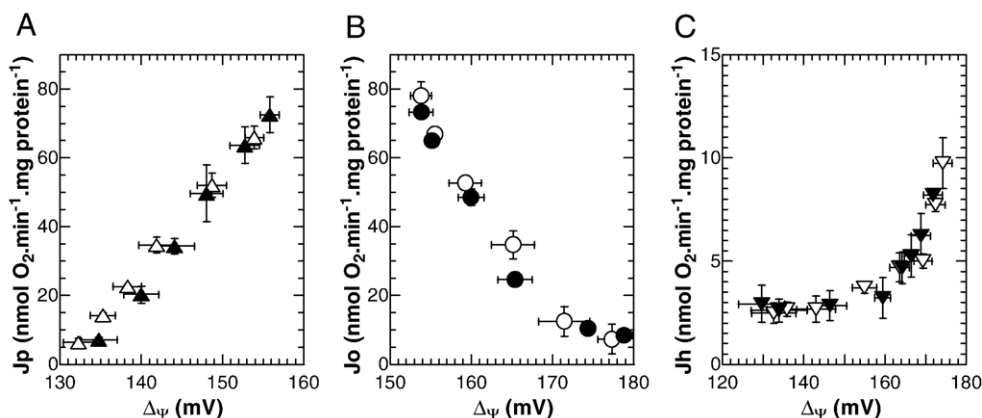

Fig. 3. Kinetics of the modules of oxidative phosphorylation; connecting intermediate is $\Delta\psi$. (A) Kinetics of the phosphorylating module determined by titration of the substrate oxidation module with 0–1.25 mM malonate. (B) Kinetics of substrate oxidation module determined by titration of the phosphorylating module with 0–0.3 μM oligomycin. (C) Kinetics of proton leak module determined by titration of the substrate oxidation module with 0–25 nM myxothiazol in the presence of 0.3 μM oligomycin. Phosphorylation flux J_p was calculated from the oxygen uptake rate corrected by proton leak rate at the same value of $\Delta\psi$; proton leak flux J_h was measured as the oxygen uptake flux in the absence of phosphorylation [25]. Data are expressed as averages from $n=6$ experiments±SEM. J_p—phosphorylation flux, J_o — oxygen uptake flux, J_h—proton leak flux; open symbols—low fat diet, closed symbols—high fat diet.
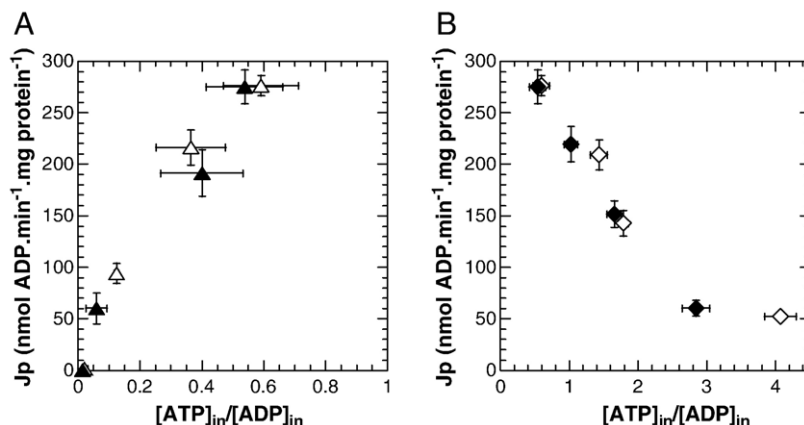
Fig. 4. Kinetics of the modules of oxidative phosphorylation, connecting intermediate is matrix ATP/ADP ratio. (A) Kinetics of ATP-consuming module determined by titration of the ATP-producing module with 0–20 nM myxothiazol. (B) Kinetics of ATP-producing module determined by titration of the ATP-consuming module with 0–1.5 μM atractyloside. Phosphorylation flux J_p was calculated from the oxygen uptake rate corrected by proton leak rate at the same value of $\Delta\psi$ multiplied by the corresponding ADP/O ratio [21]. Data are expressed as averages from $n=6$ experiments, ±SEM. J_p—phosphorylation flux, open symbols—low fat diet, closed symbols—high fat diet.

to HFD but not LFD increased accumulation of CML in the liver indicating increased oxidative stress. The observation that in HFD livers more CML, but not HNE, was found around the central vein and the portal triad, combined with the fact that HFD led to higher fasting blood glucose levels, indicates that CML formation may have resulted from increased protein glycation. The lack of HNE accumulation in livers of HFD-fed rat is in line with the fact that unsaturation index of both diets was the same, while it was shown that high levels of unsaturated fat rather than of saturated fat increased lipid-mediated oxidative stress and decreased the activity of antioxidant enzymes due to higher susceptibility of double bonds to oxidation [45].

One may expect that the alteration of intracellular environment as indicated by accumulation of LCAC and CML in liver caused by prolonged exposure to HFD may also affect mitochondria, leading to either functional impairment or adaptation through such mechanisms as changes in gene expression. So far the reports on the effects of high-fat diets and lipid overload on mitochondria metabolism have been inconclusive [8,46,47], possibly due to experimental variations, such as duration of diet exposure, lipid composition of the diet and possibly, the presence of adaptive mechanisms that prevent alterations in ATP production.

Table 4
Metabolic control of fluxes and intermediates of oxidative phosphorylation by the ANT in liver mitochondria from LFD- and HFD-fed rats

Control coefficient	LFD	HFD
$C_{ANT}^{J_o}$	0.13 ± 0.03	0.14 ± 0.03
$C_{ANT}^{J_p}$	0.14 ± 0.03	0.15 ± 0.03
$C_{ANT}^{\Delta\Psi}$	-0.09 ± 0.02	-0.11 ± 0.02
$C_{ANT}^{ATP_{in}/ADP_{in}}$	-0.46 ± 0.10	-0.56 ± 0.14
$C_{ANT}^{ATP_{out}/ADP_{out}}$	0.21 ± 0.04	0.23 ± 0.05

Averages from $n=3$, ±SEM. J_o and J_p—oxygen uptake and phosphorylation fluxes, respectively; ATP_{in}/ADP_{in} and ATP_{out}/ADP_{out} intra- and extramitochondrial ratios, respectively.

We have shown here that the oxidative capacity and efficiency of oxidative phosphorylation was not significantly affected by HFD feeding. Modular kinetic analysis revealed that kinetic properties and the expression level of the enzymes involved in the substrate oxidation and ADP phosphorylation were not significantly different in both diet groups. Furthermore, HFD feeding did not alter significantly the number of mitochondria per cell although a tendency of increase in mitochondrial copy number in livers from HFD group was observed. Thus our data now show that at least under one regimen, adaptation does not occur neither at the mitochondrial level nor in terms of a change in the number of mitochondria per cell.

In this paper we discuss the diets in terms of their fat contents, but the correlating changes in protein and carbohydrate composition should also be taken into consideration. For example, in contrast to our findings it was reported that 2 weeks of high-fat diet feeding leads to decreased oxidative capacity of liver mitochondria [47] and this discrepancy may result from the fact that protein/carbohydrate ratio in the diets was different. On the other hand, this may also indicate that although we did not find adaptation at the level of oxidative phosphorylation in response to HFD feeding, adaptation might have occurred at other levels. The lack of strong functional impairment observed in isolated mitochondria when they are separated from the cytosolic (presumably toxic) environment might be an indication that other, unassessed, adaptation processes have been present (e.g. increased levels of antioxidant enzymes, ROS scavengers, mitochondrial uncoupling proteins (UCPs)) that allowed mitochondria to maintain normal functionality. Indeed, it was shown that the functions of skeletal muscle mitochondrial remain unaltered after 36 weeks of exposure to HFD due to such adaptive changes [8].

However, the lower content of cytochromes $c+c_1$ in liver mitochondria from HFD-fed rats indicates that on the longer term HFD would have led to impaired mitochondrial function. Cytochrome c loss from the mitochondrial intermembrane space is an early step in a chain of events leading to changes in the

mitochondrial integrity (e.g. the opening of the permeability transition pore and dissipation of $\Delta\psi$) and is a signal towards apoptosis [48].

The amount and composition of dietary lipids have been shown to influence the physical properties of phospholipid bilayers [49] and the expression of UCPs that catalyze an inducible proton conductance [50], and thus may affect proton leak across the inner mitochondrial membrane. We found no significant effect of HFD on the proton leak rate and kinetics in vitro. From our experiment we can conclude that the integrity and the physical properties of the mitochondrial membrane were not affected by HFD feeding. However, it cannot be excluded that there was increased expression and activity of UCPs in liver mitochondria from HFD-fed rats in vivo, because it is possible that the procedure of isolation of the mitochondria caused removal of substances activating UCPs, e.g. fatty acids by binding to albumin present in the isolation and the reaction media.

We have shown here that HFD causes accumulation of LCAC (in particular C16:0 and C18 species) in liver. It has been hypothesized that inhibition of the mitochondrial ANT by increased concentration of intracellular LCAC caused by oversupply of lipids may be among the mechanisms underlying cellular dysfunction in obesity and type 2 diabetes. Under hyperlipidemic conditions high intracellular concentrations of LCAC are expected to lead to persistent inhibition of the ANT of various degrees resulting in lower cytosolic ATP/ADP ratio, increased cytosolic AMP levels and $\Delta\psi$, and stimulation of ROS production [19,20]. Only long chain (i.e. C>12) but not short chain acyl-CoA esters or free CoA are potent inhibitors of the ANT [51]. Saturated LCAC such as palmitoyl-CoA exert stronger effects than unsaturated LCAC [52]. Indeed, addition of palmitoyl-CoA (C16:0) to isolated rat-liver mitochondria caused the predicted changes in extra- and intramitochondrial ATP levels and $\Delta\psi$ [21], while oleoyl-CoA (C18:1) had qualitatively similar but quantitatively weaker effects (Ciapaite J. et al., unpublished data).

During prolonged exposure to increased concentrations of intracellular LCAC in vivo, mitochondria might adapt in order to protect themselves from the acute, potentially deleterious effects of LCAC by adjusting of the expression of involved enzymes or kinetics of the system in such a way, that important parameters such as $\Delta\psi$ and matrix ATP/ADP ratio are not altered. If such adaptive mechanisms counteracting the putative inhibition of ANT by LCAC would occur in vivo, one may expect to find lowered values of $\Delta\psi$ and matrix ATP/ADP ratio in vitro in isolated mitochondria from HFD rats in the absence of LCAC. This, however, was not the case; in fact, $\Delta\psi$ and ATP/ADP ratio in the matrix were quite similar in the two diet groups, suggesting that no such adaptation had taken place (it should be noted that in this experimental set-up LCAC are removed from mitochondrial preparation due to binding to albumin present in the media). We further showed that, after HFD feeding, ANT retained significant control of fluxes and intermediates that are considered important in type 2 diabetes, i.e. $\Delta\psi$ and extramitochondrial ATP/ADP ratio [19,20]. Thus, if any adaptation had escaped our observation, then this did not seem to interfere with the control of various aspects of oxidative

phosphorylation by ANT. This observation is important because for the inhibition of an enzyme (i.e. inhibition of ANT by LCAC) to have significant effect on system fluxes and intermediate levels, that enzyme must have significant control over these fluxes and intermediates.

In conclusion, long-term HFD feeding caused accumulation of LCAC in liver but did not cause adaptive changes in the kinetics of the components of the oxidative phosphorylation, resulting in increased oxidative stress as indicated by accumulation of CML. The ANT retained control of fluxes and intermediates also in liver mitochondria from HFD-fed rats, suggesting that LCAC should exert their acute effects on mitochondrial function also under conditions of persistent lipid oversupply.

Appendix A. Supplementary data

Supplementary data associated with this article can be found, in the online version, at doi:10.1016/j.bbadis.2006.10.018.

References

[1] P.A. Hansen, D.H. Han, B.A. Marshall, L.A. Nolte, M.M. Chen, M. Mueckler, J.O. Holloszy, A high fat diet impairs stimulation of glucose transport in muscle. Functional evaluation of potential mechanisms, J. Biol. Chem. 273 (1998) 26157–26163.

[2] C. Cruciani-Guglielmacci, M. Vincent-Lamon, C. Rouch, M. Orosco, A. Ktorza, C. Magnan, Early changes in insulin secretion and action induced by high-fat diet are related to a decreased sympathetic tone, Am. J. Physiol.: Endocrinol. Metab. 288 (2005) E148–E154.

[3] Y. Wang, P.Y. Wang, L.Q. Qin, G. Davaasambuu, T. Kaneko, J. Xu, S. Murata, R. Katoh, A. Sato, The development of diabetes mellitus in Wistar rats kept on a high-fat/low-carbohydrate diet for long periods, Endocrine 22 (2003) 85–92.

[4] V.T. Samuel, Z.X. Liu, X. Qu, B.D. Elder, S. Bilz, D. Befroy, A.J. Romanelli, G.I. Shulman, Mechanism of hepatic insulin resistance in non-alcoholic fatty liver disease, J. Biol. Chem. 279 (2004) 32345–32353.

[5] W.J. Bemelmans, J.D. Lefrandt, E.J. Feskens, J. Broer, J.W. Tervaert, J.F. May, A.J. Smit, Change in saturated fat intake is associated with progression of carotid and femoral intima-media thickness, and with levels of soluble intercellular adhesion molecule-1, Atherosclerosis 163 (2002) 113–120.

[6] J.A. Chavez, S.A. Summers, Characterizing the effects of saturated fatty acids on insulin signaling and ceramide and diacylglycerol accumulation in 3T3-L1 adipocytes and C2C12 myotubes, Arch. Biochem. Biophys. 419 (2003) 101–109.

[7] E.W. Kraegen, D.E. James, L.H. Storlien, K.M. Burleigh, D.J. Chisholm, In vivo insulin resistance in individual peripheral tissues of the high fat fed rat: assessment by euglycaemic clamp plus deoxyglucose administration, Diabetologia 29 (1986) 192–198.

[8] R. Sreekumar, J. Unnikrishnan, A. Fu, J. Nygren, K.R. Short, J. Schimke, R. Barazzoni, K.S. Nair, Impact of high-fat diet and antioxidant supplement on mitochondrial functions and gene transcripts in rat muscle, Am. J. Physiol.: Endocrinol. Metab. 282 (2002) E1055–E1061.

[9] L.H. Storlien, A.B. Jenkins, D.J. Chisholm, W.S. Pascoe, S. Khouri, E.W. Kraegen, Influence of dietary fat composition on development of insulin

resistance in rats. Relationship to muscle triglyceride and omega-3 fatty acids in muscle phospholipid, Diabetes 40 (1999) 280–289.

[10] P.S. Brookes, J.A. Buckingham, A.M. Tenreiro, A.J. Hulbert, M.D. Brand, The proton permeability of the inner membrane of liver mitochondria from ectothermic and endothermic vertebrates and from obese rats: correlations with standard metabolic rate and phospholipid fatty acid composition, Comp. Biochem. Physiol. B. Biochem. Mol. Biol. 119 (1998) 325–334.

[11] S. Yamaoka, R. Urade, M. Kito, Mitochondrial function in rats is affected by modification of membrane phospholipids with dietary sardine oil, J. Nutr. 118 (1988) 290–296.

[12] V. Barzanti, M. Battino, A. Baracca, M. Cavazzoni, R. Cocchi, R. Noble, M. Maranesi, E. Turchetto, G. Lenaz, The effect of dietary lipid changes on the fatty acid composition and function of liver, heart and brain mitochondria in the rat at different ages, Br. J. Nutr. 71 (1994) 193–202.

[13] E.J. McMurchie, M.Y. Abeywardena, J.S. Charnock, R.A. Gibson, Differential modulation of rat heart mitochondrial membrane-associated enzymes by dietary lipid, Biochim. Biophys. Acta 760 (1983) 13–24.

[14] J.L. Quiles, J.R. Huertas, M. Manas, J.J. Ochoa, M. Battino, J. Mataix, Dietary fat type and regular exercise affect mitochondrial composition and function depending on specific tissue in the rat, J. Bioenerg. Biomembr. 33 (2001) 127–134.

[15] K.F. Petersen, D. Befroy, S. Dufour, J. Dziura, C. Ariyan, D.L. Rothman, L. DiPietro, G.W. Cline, G.I. Shulman, Mitochondrial dysfunction in the elderly: possible role in insulin resistance, Science 300 (2003) 1140–1142.

[16] K.F. Petersen, S. Dufour, D. Befroy, R. Garcia, G.I. Shulman, Impaired mitochondrial activity in the insulin-resistant offspring of patients with type 2 diabetes, N. Engl. J. Med. 350 (2004) 664–671.

[17] V.B. Ritov, E.V. Menshikova, J. He, R.E. Ferrell, B.H. Goodpaster, D.E. Kelley, Deficiency of subsarcolemmal mitochondria in obesity and type 2 diabetes, Diabetes 54 (2005) 8–14.

[18] J. Knudsen, T.B. Neergaard, B. Gaigg, M.V. Jensen, J.K. Hansen, Role of acyl-CoA binding protein in acyl-CoA metabolism and acyl-CoA-mediated cell signaling, J. Nutr. 130 (2000) 294S–298S.

[19] S.J. Bakker, R.G. IJzerman, T. Teerlink, H.V. Westerhoff, R.O. Gans, R.J. Heine, Cytosolic triglycerides and oxidative stress in central obesity: the missing link between excessive atherosclerosis, endothelial dysfunction, and β-cell failure? Atherosclerosis 148 (2000) 17–21.

[20] S.J. Bakker, R.O. Gans, J.C. ter Maaten, T. Teerlink, H.V. Westerhoff, R.J. Heine, The potential role of adenosine in the pathophysiology of the insulin resistance syndrome, Atherosclerosis 155 (2001) 283–290.

[21] J. Ciapaite, G. van Eikenhorst, S.J. Bakker, M. Diamant, R.J. Heine, M.J. Wagner, H.V. Westerhoff, K. Krab, Modular kinetic analysis of the adenine nucleotide translocator-mediated effects of palmitoyl-CoA on the oxidative phosphorylation in isolated rat liver mitochondria, Diabetes 54 (2005) 944–951.

[22] J. Ciapaite, S.J. Bakker, M. Diamant, G. van Eikenhorst, R.J. Heine, H.V. Westerhoff, K. Krab, Metabolic control of mitochondrial properties by adenine nucleotide translocator determines palmitoyl-CoA effects: implications for a mechanism linking obesity and type 2 diabetes, FEBS. J. 273 (2006) 5288–5302.

[23] V. Mildaziene, Z. Nauciene, R. Baniene, J. Grigiene, Multiple effects of 2,2,5,5-tetrachlorbiphenyl on oxidative phosphorylation in rat liver mitochondria, Toxicol. Sci. 65 (2002) 220–227.

[24] M.M. Bradford, A rapid and sensitive method for the quantification of microgram quantities of protein utilizing the principle of protein-dye binding, Anal. Biochem. 72 (1976) 248–254.

[25] R.P. Hafner, G.C. Brown, M.D. Brand, Analysis of the control of respiration rate, phosphorylation rate, proton leak rate and protonmotive force in isolated mitochondria using the 'top-down' approach of metabolic control theory, Eur. J. Biochem. 188 (1990) 313–319.

[26] P.C. Hinkle, Measurement of ADP/O ratios, in: G.C. Brown, C.E. Cooper (Eds.), Bioenergetics—A practical approach, IRL Press, Oxford, 1995, pp. 5–6.

[27] K. Krab, M.J. Wagner, A.M. Wagner, I.M. Moller, Identification of the site where the electron transfer chain of plant mitochondria is stimulated by electrostatic charge screening, Eur. J. Biochem. 267 (2000) 869–876.

[28] B. Chance, G.R. Williams, Respiratory enzymes in oxidative phosphorylation: II. Difference spectra, J. Biol. Chem. 217 (1955) 395–407.

[29] B.F. van Gelder, On cytochrome c oxidase. I. The extinction coefficients of cytochrome a and cytochrome a_3, Biochim. Biophys. Acta 118 (1966) 36–46.

[30] C.W. van den Bergen, A.M. Wagner, K. Krab, A.L. Moore, The relationship between electron flux and the redox poise of the quinone pool in plant mitochondria. Interplay between quinol-oxidizing and quinone-reducing pathways, Eur. J. Biochem. 226 (1994) 1071–1078.

[31] P.R. Jensen, H.V. Westerhoff, O. Michelsen, Excess capacity of H^+-ATPase and inverse respiratory control in *Escherichia coli*, EMBO J. 12 (1993) 1277–1282.

[32] Y. Zhang, K. Ma, S. Song, M.B. Elam, G.A. Cook, E.A. Park, Peroxisomal proliferator-activated receptor-gamma coactivator-1 alpha (PGC-1 alpha) enhances the thyroid hormone induction of carnitine palmitoyltransferase I (CPT-I alpha), J. Biol. Chem. 279 (2004) 53963–53971.

[33] K. Szuhai, J. Ouweland, R. Dirks, M. Lemaitre, J. Truffert, G. Janssen, H. Tanke, E. Holme, J. Maassen, A. Raap, Simultaneous A8344G heteroplasmy and mitochondrial DNA copy number quantification in myoclonus epilepsy and ragged-red fibers (MERRF) syndrome by a multiplex molecular beacon based real-time fluorescence PCR, Nucleic Acids Res. 29 (2001) E13.

[34] C.G. Schalkwijk, A. Baidoshvili, C.D. Stehouwer, V.W. van Hinsbergh, H.W. Niessen, Increased accumulation of the glycoxidation product Nepsilon-(carboxymethyl)lysine in hearts of diabetic patients: generation and characterisation of a monoclonal anti-CML antibody, Biochim. Biophys. Acta 1636 (2004) 82–89.

[35] S. Toyokuni, N. Miyake, H. Hiai, M. Hagiwara, S. Kawakishi, T. Osawa, K. Uchida, The monoclonal antibody specific for the 4-hydroxy-2-nonenal histidine adduct, FEBS Lett. 359 (1995) 189–191.

[36] R. Heinrich, T.A. Rapoport, A linear steady-state treatment of enzymatic chains. General properties, control and effector strength, Eur. J. Biochem. 42 (1974) 89–95.

[37] H.V. Westerhoff, K. van Dam, Thermodynamics and control of free-energy transduction, Elsevier Publishers, Amsterdam, 1987.

[38] D.M. Ouwens, C. Boer, M. Fodor, P. de Galan, R.J. Heine, J.A. Maassen, M. Diamant, Cardiac dysfunction induced by high-fat diet is associated with altered myocardial insulin signalling in rats, Diabetologia 48 (2005) 1229–1237.

[39] S. Soboll, H.J. Seitz, H. Sies, B. Ziegler, R. Scholz, Effect of long-chain fatty acyl-CoA on mitochondrial and cytosolic ATP/ADP ratios in the intact liver cell, Biochem. J. 220 (1984) 371–376.

[40] O. Larsson, J.T. Deeney, R. Branstrom, P.O. Berggren, B.E. Corkey, Activation of the ATP-sensitive K+ channel by long chain acyl-CoA. A role in modulation of pancreatic beta-cell glucose sensitivity, J. Biol. Chem. 271 (1996) 10623–10626.

[41] F. Morel, G. Lauquin, J. Lunardi, J. Duszynski, P.V. Vignais, An appraisal of the functional significance of the inhibitory effect of long chain acyl-CoAs on mitochondrial transports, FEBS Lett. 39 (1974) 133–138.

[42] M.X. Fu, K.J. Wells-Knecht, J.A. Blackledge, T.J. Lyons, S.R. Thorpe, J.W. Baynes, Glycation, glycoxidation, and cross-linking of collagen by glucose. Kinetics, mechanisms, and inhibition of late stages of the Maillard reaction, Diabetes 43 (1994) 676–683.

[43] M.X. Fu, J.R. Requena, A.J. Jenkins, T.J. Lyons, J.W. Baynes, S.R. Thorpe, The advanced glycation end product, Nepsilon-(carboxymethyl) lysine, is a product of both lipid peroxidation and glycoxidation reactions, J. Biol. Chem. 271 (1996) 9982–9986.

[44] A. Benedetti, M. Comporti, H. Esterbauer, Identification of 4-hydroxynonenal as a cytotoxic product originating from the peroxidation of liver microsomal lipids, Biochim. Biophys. Acta 620 (1980) 281–296.

[45] R.M. Slim, M. Toborek, B.A. Watkins, G.A. Boissonneault, B. Hennig, Susceptibility to hepatic oxidative stress in rabbits fed different animal and plant fats, J. Am. Coll. Nutr. 15 (1996) 289–294.

[46] R. De Schrijver, O.S. Privett, Energetic efficiency and mitochondrial function in rats fed trans fatty acids, J. Nutr. 114 (1984) 1183–1191.

[47] S. Iossa, L. Lionetti, M.P. Mollica, R. Crescenzo, M. Botta, A. Barletta, G. Liverini, Effect of high-fat feeding on metabolic efficiency and mitochondrial oxidative capacity in adult rats, Br. J. Nutr. 90 (2003) 953–960.

[48] X. Liu, C.N. Kim, J. Yang, R. Jemmerson, X. Wang, Induction of apoptotic

program in cell-free extracts: requirement for dATP and cytochrome c, Cell 86 (1996) 147–157.

[49] J.J. Ramsey, M.E. Harper, S.J. Humble, E.K. Koomson, J.J. Ram, L. Bevilacqua, K. Hagopian, Influence of mitochondrial membrane fatty acid composition on proton leak and H2O2 production in liver, Comp. Biochem. Physiol. B. Biochem. Mol. Biol. 140 (2005) 99–108.

[50] A. Rashid, T.C. Wu, C.C. Huang, C.H. Chen, H.Z. Lin, S.Q. Yang, F.Y. Lee, A.M. Diehl, Mitochondrial proteins that regulate apoptosis and necrosis are induced in mouse fatty liver, Hepatology 29 (1999) 1131–1138.

[51] A. Shug, E. Lerner, C. Elson, E. Shrago, The inhibition of adenine nucleotide translocase activity by oleoyl CoA and its reversal in rat liver mitochondria, Biochem. Biophys. Res. Commun. 43 (1971) 557–563.

[52] E. Shrago, A. Shug, C. Elson, T. Spennetta, C. Crosby, Regulation of metabolic transport in rat and guinea pig liver mitochondria by long chain fatty acyl coenzyme A esters, J. Biol. Chem. 249 (1974) 5269–5274.